Single-conductor co-planar quasi-symmetry unequal power divider based on spoof surface plasmon polaritons of bow-tie cells

Yongle Wu, Mingxing Li, Guangyou Yan, Li Deng, Yuanan Liu, and Zabih Ghassemlooy

Citation: AIP Advances **6**, 105110 (2016); doi: 10.1063/1.4966051
View online: http://dx.doi.org/10.1063/1.4966051
View Table of Contents: http://scitation.aip.org/content/aip/journal/adva/6/10?ver=pdfcov
Published by the AIP Publishing

Single-conductor co-planar quasi-symmetry unequal power divider based on spoof surface plasmon polaritons of bow-tie cells

Yongle Wu,[1,a,b] Mingxing Li,[1,a] Guangyou Yan,[2] Li Deng,[3] Yuanan Liu,[1] and Zabih Ghassemlooy[4]

[1]*Beijing Key Laboratory of Work Safety Intelligent Monitoring, School of Electronic Engineering, Beijing University of Posts and Telecommunications, P.O. Box. 282, 100876 Beijing, China*

[2]*School of Physical Electronics, University of Electronic Science and Technology of China, 610054 Chengdu, Sichuan, China*

[3]*Beijing Key Laboratory of Network System Architecture and Convergence, School of Information and Communication Engineering, Beijing University of Posts and Telecommunications, 100876 Beijing, China*

[4]*Optical Communications Research Group, NCRLab, Faculty of Engineering and Environment, Northumbria University, Newcastle upon Tyne NE1 8ST, United Kingdom*

(Received 2 July 2016; accepted 11 October 2016; published online 18 October 2016)

In this paper, the spoof surface plasmon polaritons (SSPPs) transmission line (TL) of periodical grooved bow-tie cells is proposed. The complex propagation constant and characteristic impedance of the SSPPs TLs and microstrip lines (MLs) are extracted using the analytical method of generalized lossy TL theory. The properties of the SSPPs TLs with different substrates and the same geometrical configuration are experimented. Then, for comparison, two ML counterparts are also experimented, which shows that the SSPPs TL is less sensitive to the thickness, dielectric constant and loss tangent of the chosen substrate below the cutoff frequency, compared with the ML ones. The single-conductor co-planar quasi-symmetry unequal power divider based on this SSPPs TL is presented in microwave frequencies. For experimental validation, the 0-dB, 2-dB, and 5-dB power dividers are designed, fabricated, and measured. Both simulated and measured results verify that the unequal power divider is a flexible option, which offers massive advantages including single-conductor co-planar quasi-symmetry structures, wide-band operation, and convenient implementations of different power-dividing ratios. Hence, it can be expected that the proposed unequal power dividers will inspire further researches on SSPPs for future design of novel planar passive and active microwave components, circuits and systems. [http://dx.doi.org/10.1063/1.4966051]

I. INTRODUCTION

Surface plasmon polaritons (SPPs) are waves that propagate along the metal's surface due to the interaction of free electrons and photons in the field of optics, which has been explored extensively in subwavelength optics, data storage, microscopy, and biosensor.[1] Despite metals are presented as perfectly electric conductors (PECs) instead of plasma with negative permittivity at lower frequencies, the mimicking surface plasmons or spoof surface plasmon polaritons (SSPPs) propagating along a perfectly conducting surface can also be achieved by drilling an array of holes or corrugating with a periodic array of radial grooves.[2,3] Consequently, a large number of studies on TLs that can support

[a]Yongle Wu and Mingxing Li contributed equally to this work.

[b]wuyongle138@gmail.com.

SSPPs have been performed over the last years,[4–11] in which SSPPs are structured by ML with periodic holes, corrugated metal surface with underlayer metal, complementary symmetric grooves, comb-shaped cells, etc. For characterizing the SSPPs, equivalent circuit model of SSPPs unit cell[12] and analysis of loss feature about the SSPPs TL based on the perturbation method[13] are already proposed, nevertheless, extraction of the complex propagation constant and the characteristic impedance is still an inevitable obstacle in further expanding the range of SSPPs applications.

Recently, numerous researches on a wide range of components or devices utilizing SSPPs have been reported. In order to achieve frequency-selective SSPPs in the microwave and terahertz frequencies, high performance wideband filters exploiting the high confinement property of the SSPPs mode have been proposed,[14–16] and tunable rejections can be achieved by adding electrically resonant metamaterials near the SSPPs TL.[17] Additionally, directional couplers,[18–20] power dividers[18,21] and feeding network for the antenna array[22] have been designed. It is suggested that the SSPPs have enormous potential of building such a circuit or system at lower frequency bands. However, to the best of our knowledge, there are no published reports on unequal SSPPs-based power dividers with flexible power-division ratios, which will be necessary in asymmetric power amplifiers,[23] passive and active antenna arrays,[24] high-performance radar front-ends,[25] etc. Therefore, the development of novel unequal SSPPs-based power dividers is prior to the implementation of the SSPPs-based microwave front-ends including power amplifiers and antenna arrays.

In this paper, the SSPPs TL of periodical grooved bow-tie cells is proposed. The complex propagation constant and characteristic impedance of the SSPPs TLs and MLs are extracted using the analytical method of generalized lossy TL theory. The properties of the SSPPs TLs with different substrates and the same geometrical configuration are experimented. For comparison, two ML counterparts are also experimented, which shows that the SSPPs TL is less sensitive to the thickness, dielectric constant and loss tangent of the chosen substrate below the cutoff frequency, compared with the ML ones. Then, we present a single-conductor co-planar quasi-symmetry unequal power divider with different power-dividing ratios. For experimental validation, the 0-dB, 2-dB, and 5-dB power dividers are designed, fabricated, and measured. Both simulated and measured results show that the SSPPs-based unequal power dividers offer several advantages: 1) single-conductor co-planar quasi-symmetry structures, 2) easy implementations of different power-dividing ratios, 3) wide-band operation (3-8 GHz and almost the fractional bandwidth of 91%), and 4) the external performances are less sensitive to the thickness, dielectric constant and loss tangent of the chosen substrate below the cutoff frequency. Therefore, it can be believed that the proposed SSPPs-based unequal power divider will be a flexible alternative for controllable output power division and it will play an important role in further developments and applications of SSPPs-based circuits and systems in microwave and terahertz frequencies.

II. DESIGN OF SSPPS TL

One of the important features of SSPPs TL is SSPPs waves can propagate along the periodically structured metal surfaces in microwave frequencies. The propagation characteristics of the SSPPs can be controlled by the metal geometry, such as array of drilled holes,[2,9] periodically corrugated metal surface,[4–7] complementary symmetric grooves,[8] and trapezoidal grooves.[10] In this paper, the SSPPs TL of periodical grooved bow-tie cells with easy adjustment of more parameters, enhanced confinement of surface waves on the two edges of the symmetrical bow-tie metallic cells, and flexibility of building power dividers is proposed. The proposed single-conductor SSPPs TL of 20-unit bow-tie cells is depicted in Figure 1(a). The waves propagating along the SSPPs TL are realized using bow-tie cells, and broadband transition with quarter elapse and gradient SSPPs line is used to achieve high-efficiency conversion between coplanar waveguide (CPW) and SSPPs TL.

In the proposed bow-tie cell, the widths (c_1 and c_2), depth (l_3) and length (w_3) of a side of the void square have major influence on the dispersion relations and confinement ability of SSPPs waves. The dispersion curves of the SSSP unit cells with different parameters and MLs on substrates FR4 and Di880, which are solved by the eigenmode solver of CST Microwave Studio, are plotted in Figures 1(b) and (c). When c_1 = 2 mm, c_2 = 2 mm, w_3 = 0 mm, and l_3 = 4 mm, the bow-tie cell becomes normal H-shaped structure in Refs. 3,11,16,17,19–21. As shown in Figures 1(b) and (c),

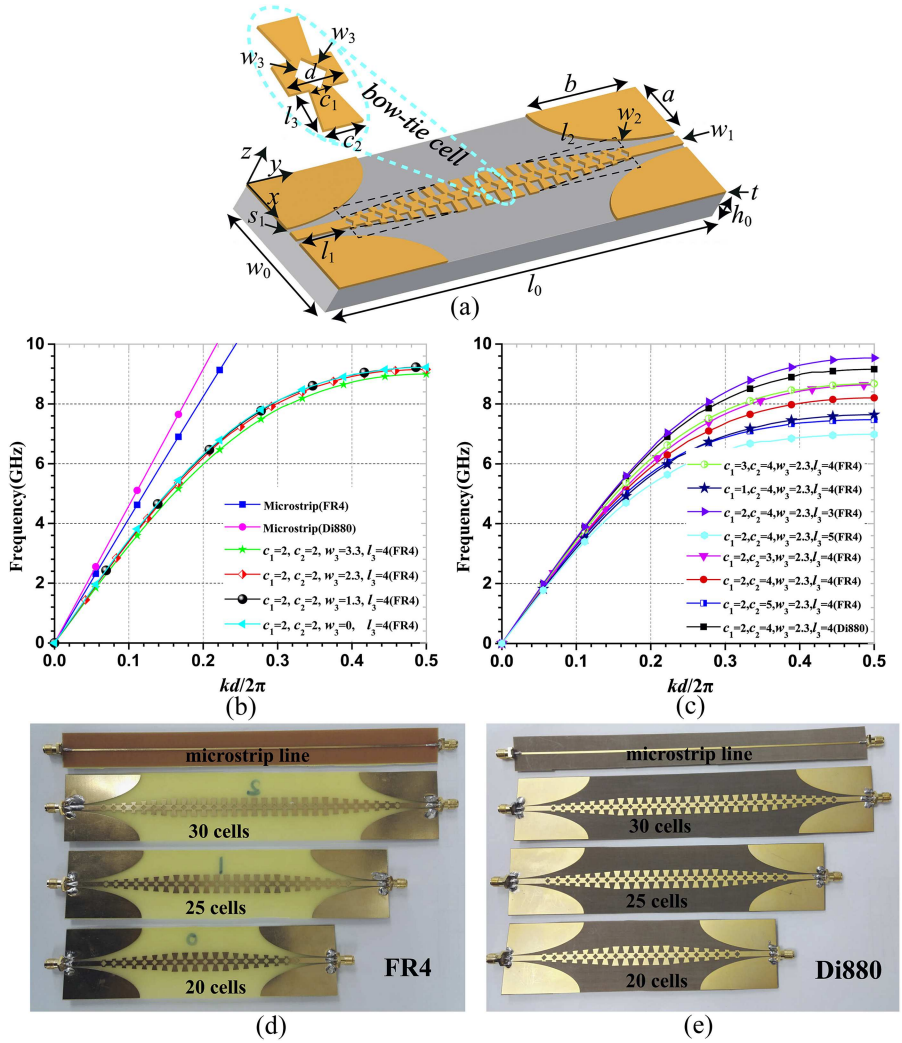

FIG. 1. (a) The structure of 20 unit cells SSPPs TL (w_0 = 40 mm, l_0 =160 mm, c_1 = 2 mm, c_2 = 4 mm, d = 6 mm, w_3 = 2.33 mm, and l_3 = 4 mm). To facilitate the measurements, a broadband transition from CPW to SSPPs TL with quarter elapse and gradient SSPPs line is designed (a = 45 mm, b = 18.225 mm, w_1 = 3 mm, s_1 = 0.275 mm, l_1 = 20 mm, w_2 = 3.5 mm, and l_2 = 42 mm). (b) and (c) Dispersion relations of the bow-tie cells with different parameters and the MLs. (d) Photograph of the SSPPs TLs with 20, 25 and 30 bow-tie cells and the ML fabricated on FR4. (e) Photograph of the SSPPs TLs with 20, 25 and 30 bow-tie cells and the ML fabricated on Di880. Geometrical configurations of the photographs (d) and (e) are the same (the length and width of the MLs are 220 mm and 1.17 mm, respectively).

the dispersion curves shift down with the width (c_1) decreasing or the width (c_2), the depth (l_3), and the length (w_3) of a side of the void square increasing. We can obtain a stronger field confinement and the cutoff frequencies by optimizing the parameters c_1, c_2, l_3 and w_3. Therefore, final geometric parameters of the bow-tie cell are set as c_1 = 2 mm, c_2 = 4 mm, d = 6 mm, w_3 = 2.33 mm, and l_3 = 4 mm. The other dimensions are w_0 = 40 mm, l_0 = 160 mm, a = 45 mm, b = 18.225 mm, w_1= 3 mm, s_1= 0.275, l_1 = 20 mm, w_2 = 3.5 mm and l_2 = 42 mm. The SSPPs TLs are simulated and fabricated on two different dielectric substrates FR4 and Di880 with the same geometrical configuration. The substrate thickness h_0, dielectric constant ε_r, loss tangent tan δ, and metal thickness t are 0.6 mm, 4.4, 0.02, and 0.035 mm for FR4, and 0.508 mm, 2.2, 0.0009, and 0.035 mm for Di880, respectively. The final SSPPs TLs fabricated on the dielectric substrates FR4 and Di880, compared to the MLs, show frequency saturation beyond 8.2 GHz and 9.16 GHz, respectively. The Figures 1(d) and (e) show fabricated photographs of the SSPPs TLs and MLs. To measure the scattering parameters conveniently, the standard SMA connectors are welded on input/output ports of all samples. Figure 2 illustrates the simulated amplitudes of electric field distributions of 25 bow-tie cells SSPPs

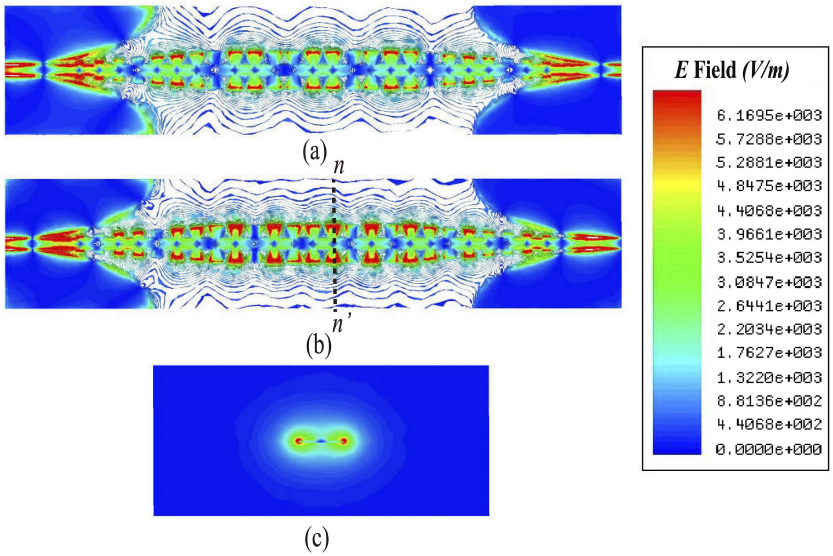

FIG. 2. The simulated electric field distributions with the color scale ranging from dark red (highest amplitude) to dark blue (lowest amplitude). The amplitude of electric field evaluated in the *x*-*y* plane along the 25 cells SSPPs TL at (a) 5 GHz, and (b) 7 GHz. (c) The electric field distributions on the cross-section of the bow-tie cell (the black line *n*-*n'* in (b)).

TL at 5 GHz and 7 GHz. It can be seen that high confinement of the electric energy on the surface and two edges of the symmetrical bow-tie metallic cells is realized.

III. ANALYSIS of SSPPs TLs and MLs

For comparison, we fabricate several SSPPs TLs with different numbers of bow-tie cells and MLs on two different types of substrates. The measured scattering parameters of 20-, 25- and 30-cells SSPPs TLs are in good agreement with the simulated results from 3 to 8 GHz, as shown in Figures 3(a), (b) and (c). Note that the proposed SSPPs TLs are less sensitive to the thickness, dielectric constant and loss tangent of the chosen substrate below the frequency of 8 GHz compared to the ML in Figure 3. The numbers of unit cells (i.e. different length) and substrate types of SSPPs TLs have little effect on the reflection and transmission coefficients, namely, S_{11} and S_{21}, respectively. However, the substrate type of ML has the bigger effect on S_{11} and S_{21}, as shown in Figure 3(d). This is due to the variation of the characteristic impedance, as a result of the substrate having different thickness and dielectric constant. Compared to the simulated results, the measured S_{11} and S_{21} of MLs change obviously within the operating frequency, because both the dielectric constant and dielectric loss vary with the frequency. Therefore, if the proposed SSPPs TLs are applied to the microwave components, circuits, and systems, they will have a special and inherent feature, namely, the external performances are less sensitive to the thickness, dielectric constant and loss tangent of the chosen substrate below the cutoff frequency.

The attenuation phenomenon is one of the important features of the SSPPs TLs, thus the generalized lossy TL theory is utilized to represent the properties of the two-port single-conductor co-planar SSPPs TLs accurately. Unlike the lossless TL theory, the generalized lossy TL theory is widely applied in microwave engineering. The complex propagation constant γ and the characteristic impedance Z_C can be determined by the following equations:[26,27]

$$\gamma = \alpha + j\beta = \cosh^{-1}\left(\frac{(1+S_{11})(1-S_{22})+S_{12}S_{21}}{2S_{12}}\right)\Big/L, \tag{1}$$

$$Z_C = R_C + jX_C = R_0\sqrt{\frac{(1+S_{11})(1+S_{22})-S_{12}S_{21}}{(1-S_{11})(1-S_{22})-S_{12}S_{21}}}, \tag{2}$$

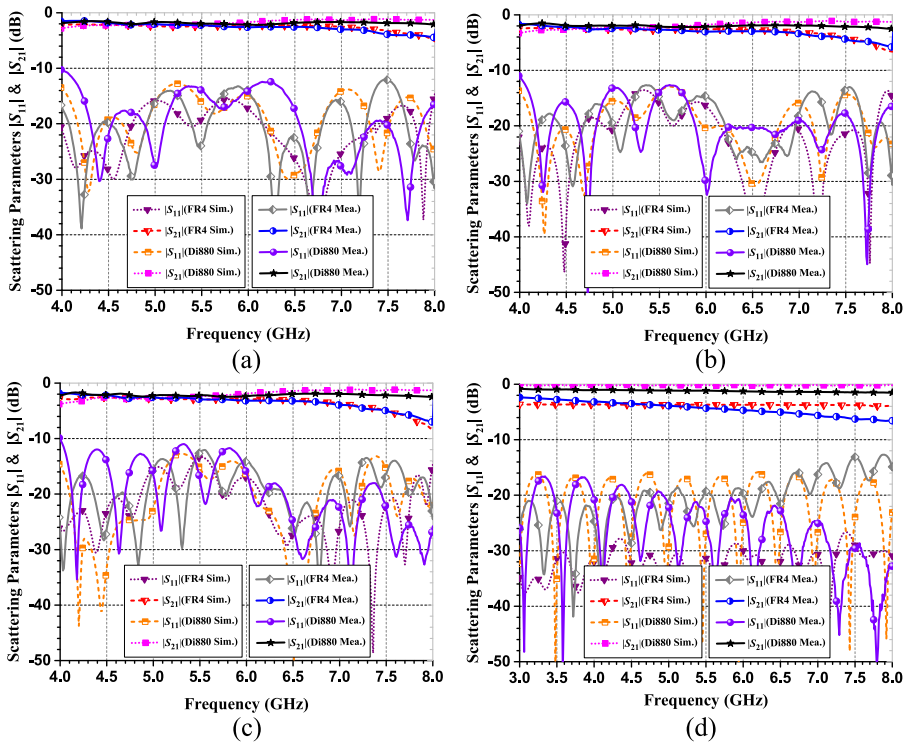

FIG. 3. Comparison of SSPPs TLs with different number of unit cells and MLs. The simulated and measured scattering parameters of SSPPs TLs fabricated on FR4 and Di880 with (a) 20 unit cells, (b) 25 unit cells, and (c) 30 unit cells. (d) The simulated and measured scattering parameters of MLs fabricated on FR4 and Di880 (the length and width are 220 mm and 1.17 mm, respectively).

where $S_{ij(=1,2)}$ can be the simulated or measured scattering parameters while α, β, R_C, X_C, R_0, and L are the attenuation constant, phase constant, real and imaginary parts of the characteristic impedance, the port impedance, and the length of TL, respectively.

It can be observed from Figure 4(a), the predicted attenuation constant α of FR4-based SSPPs TL is much smaller than that of FR4-based MLs. In addition, although the used substrates change from Di880 to FR4 for SSPPs TL, the variations of attenuation constant α and phase constant β of the SSPPs TLs are less obvious than MLs from 3 to 6 GHz. Figure 4(b) shows the complex characteristic impedance (i.e., the real part R_C and the imaginary part X_C) of SSPPs TLs and MLs with the substrates

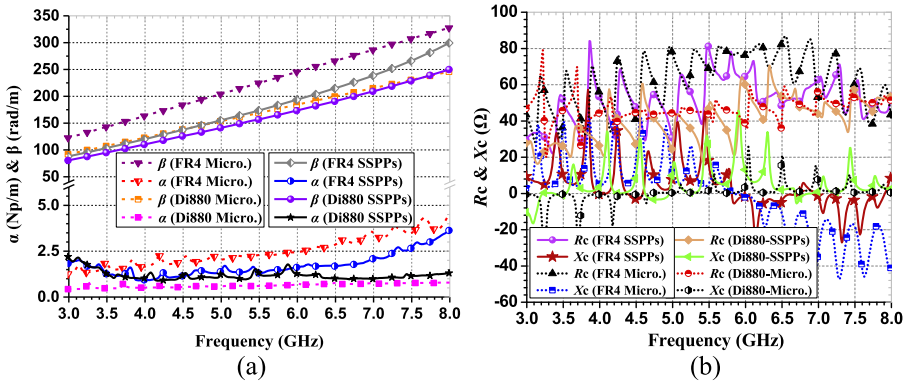

FIG. 4. The calculated complex propagation constants and complex characteristic impedances of SSPPs TLs and MLs fabricated on FR4 and Di880. (a) The attenuation constant α, phase constant β. (b) Real part R_C and imaginary part X_C of characteristic impedance.

of FR4 and Di880. Similarly, compared to MLs, the variations of complex characteristic impedance of SSPPs TL are less obvious when two different substrates are applied.

IV. DESIGN of SSPPs-BASED POWER DIVIDERS WITH VARIOUS UNEQUAL POWER DIVISIONS

According to the coupled mode theory, when two waveguides with the same propagation constant are placed adjacently, the electromagnetic energy can be efficiently coupled from one waveguide to another. Therefore, it is hopeful to design a power divider with different power-dividing ratios by constructing symmetry or quasi-symmetry structures. The single-conductor co-planar power divider with different power-dividing ratios using the proposed SSPPs TL is presented. The design procedures of the unequal power dividers can be summarized as follows. 1) Determine the operating frequency and the cutoff frequency. Choose the values of dielectric constant, thickness, and loss tangent of the material substrate. Then, determine parameters of the bow-tie cell according to dispersion curves. 2) Determine the number of SSPPs cells, and design the broadband transition for high-efficiency conversion between the CPW and SSPPs TL. 3) Duplicate and rotate one-half of the SSPPs TL along the z-axis, and determine the size of two interfaces connecting input and output (the core part of the power divider). 4) Simulate and measure the total scattering parameters of the proposed power divider.

In order to demonstrate the flexible unequal power-division feature of this proposed power divider, three cases with different power-division ratios are designed and fabricated on FR4. The schematic configuration of these power dividers are depicted in Figure 5. Figure 5(a) shows the diagram of equal power divider case, one-half of 20 unit cells SSPPs TL (Fig. 1 (a)) of length d = 80 mm is duplicated and rotated the angle θ of 150^o along the z-axis, and cut by the blue dashed triangle to divide the electromagnetic energy into two outputs. By cutting the blue dashed trapezium T and changing the shape of the blue dashed triangle, different power-dividing ratios or coupling coefficients of the proposed SSPPs-based power divider are obtained. The core parts of the 0-, 2-, and 5-dB power dividers are shown in Figures 5(b), (c) and (d). It can be seen from the Figure 6 that flexible alternatives for output power division are achieved and the measured power-division ratios are about 0, 2 and 5 dB, respectively. The measured results verify that the implementations of different power-dividing ratios of the proposed SSPPs-based power divider using a single-conductor co-planar quasi-symmetry structure can be easily and conveniently accomplished, which is essentially different from the ML-based unequal power dividers.[28] In addition, simulated and measured results show that the proposed SSPPs-based unequal power dividers can provide wide-band operation and the operating 10 dB return-loss band is about from 3 to 8 GHz (i.e. the fractional bandwidth is almost 91%).

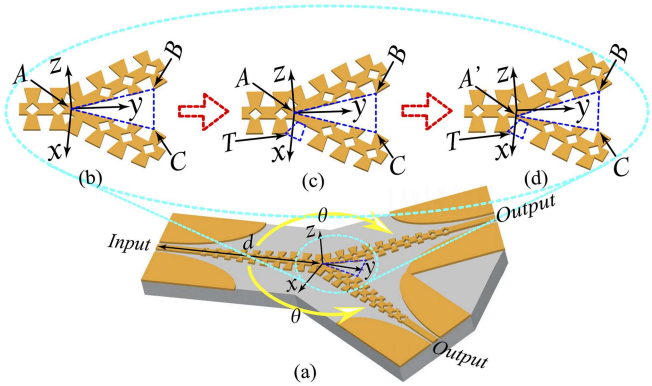

FIG. 5. Geometry configuration of the equal and unequal power dividers. (a) The 0-dB equal power divider. The left half part of the 20 cells SSPPs TL in Fig. 1 (a) (length d = 80 mm) is duplicated and rotated θ = 150 degree along Z axis, and cut by the blue dashed triangle. (b) The core part of 0-dB equal power divider. Coordinates of points A, B and C of the blue dashed triangle are (0 mm, 0 mm, 0 mm), (-5.24 mm, 19.06 mm, 0 mm), and (5.24 mm, 19.06 mm, 0 mm), respectively. (c) The core part of 2-dB unequal power divider. Coordinates of points of the blue dashed triangle stay unchanged and cut one side of bow-tie cell (blue dashed trapezium T). (d) The core part of 5-dB unequal power divider. Coordinates of point A is moved from (0 mm, 0 mm, 0 mm) to point A' (1.4 mm, 0 mm, 0 mm), and one side of bow-tie cell (blue dashed trapezium T) is cut.

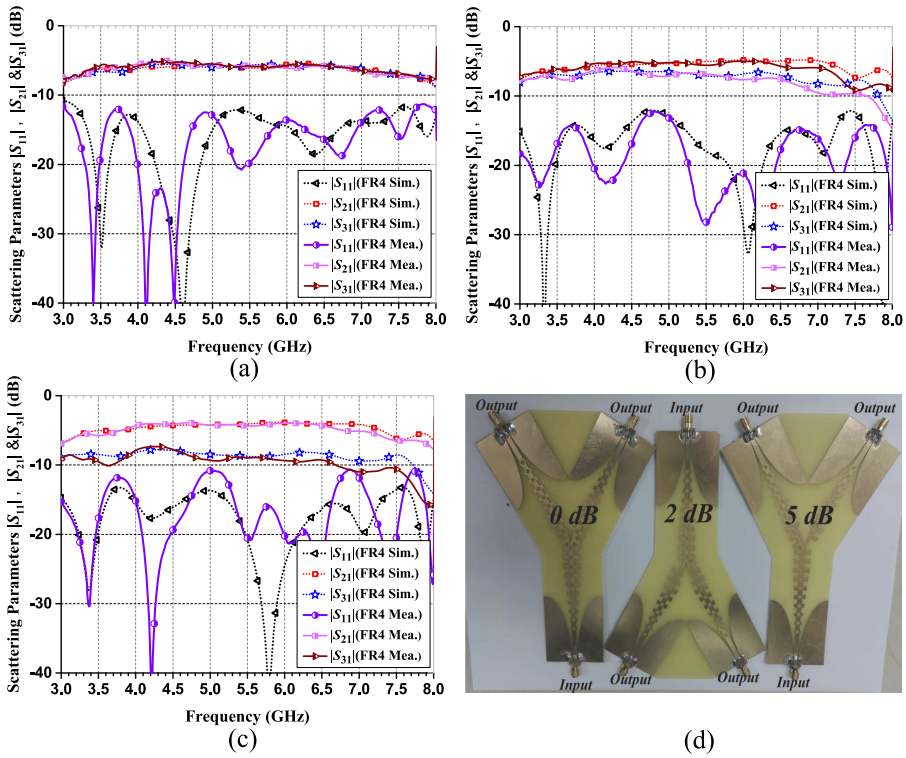

FIG. 6. Simulated and measured scattering parameters and the photograph of the power dividers with different power-dividing ratios. (a) 0-dB equal power divider, (b) 2-dB unequal power divider, and (c) 5-dB unequal power divider. (d) The photograph of the SSPPs-based power dividers fabricated on FR4.

V. CONCLUSIONS

In summary, we have proposed a new single-conductor co-planar SSPPs TL with novel periodical grooved bow-tie cells for the first time. By utilizing the generalized lossy TL theory, the complex propagation constant and characteristic impedance of the SSPPs TLs are effectively and conveniently extracted to analyze the lossy feature of the proposed SSPPs TLs. We also compare the properties of the SSPPs TLs and MLs with two different substrates in the case of the same geometrical configuration. We further verify that SSPPs TLs are less sensitive to the thickness, dielectric constant and loss tangent of the chosen substrate below the cutoff frequency, which is a clear advantage. Finally, a novel single-conductor co-planar quasi-symmetry unequal power divider based on the proposed SSPPs TL is investigated. The key advantages of the proposed SSPPs-based unequal power dividers include (i) the external performances are less sensitive to the thickness, dielectric constant and loss tangent of the chosen substrate below the cutoff frequency, (ii) single-conductor co-planar quasi-symmetry structures, (iii) wide-band operation (the fractional bandwidth of 91%), and (iv) simple implementation of different power-dividing ratios. We show that different wide-band power-dividing ratios of the SSPPs-based power divider can be readily designed and implemented using a single-conductor co-planar quasi-symmetry structure, which would lead to future implementation of other novel single-conductor co-planar passive and active microwave components, circuits and systems based on the SSPPs TLs.

VI. METHODS

Numerical simulations of SSPPs TLs and E-fields are performed by the commercial software Ansoft HFSS, and dispersion curves are performed by the commercial software CST Microwave Studio. Two types of substrates FR4 and Di880 are chosen for the simulation model and experimental

fabrication, and the scattering parameters of the fabricated samples are measured using the four-port Rohde&Schwarz Vector Network Analyzer (ZVA 8).

ACKNOWLEDGMENTS

This work was supported by National Basic Research Program of China (973 Program) (No. 2014CB339900), and National Natural Science Foundations of China (No. 61422103, No. 61671084, No. 61327806, and No. 61201027).

[1] W. L. Barnes, A. Dereux, and T. W. Ebbesen, "Surface plasmon subwavelength optics," Nature **424**, 824–830 (2003).
[2] J. B. Pendry, L. Martin-Moreno, and F. J. Garcia-Vidal, "Mimicking surface plasmons with structured surfaces," Science **305**, 847–848 (2004).
[3] S. A. Maier, S. R. Andrews, L. Martin-Moreno, and F. J. Garcia-Vidal, "Terahertz surface plasmon-polariton propagation and focusing on periodically corrugated metal wires," Phys. Rev. Lett. **97**, 176805 (2006).
[4] T. Jiang, L. Shen, X. Zhang, and L. X. Ran, "High-order modes of spoof surface plasmon polaritons on periodically corrugated metal surfaces," Prog. Electromagn. Res. M **8**, 91–102 (2009).
[5] X. Liu, Y. Feng, B. Zhu, J. Zhao, and T. Jiang, "High-order modes of spoof surface plasmonic wave transmission on thin metal film structure," Opt. Express **21**, 31155–31165 (2013).
[6] X. Shen, T. J. Cui, D. Martin-Cano, and F. J. Garcia-Vidal, "Conformal surface plasmons propagating on ultrathin and flexible films," Proc. Natl. Acad. Sci. **110**, 40–45 (2013).
[7] Z. Liao, J. Zhao, B. C. Pan, X. P. Shen, and T. J. Cui, "Broadband transition between microstrip line and conformal surface plasmon waveguide," J. Appl. Phys. **47**, 315103 (2014).
[8] X. Gao, L. Zhou, and T. J. Cui, "Odd-mode surface plasmon polaritons supported by complementary plasmonic metamaterial," Sci. Rep. **5**, 9250 (2015).
[9] L. Liu, Z. Li, B. Xu, P. Ning, C. Chen, J. Xu, X. Chen, and C. Gu, "Dual-band trapping of spoof surface plasmon polaritons and negative group velocity realization through microstrip line with gradient holes," Appl. Phys. Lett. **107**, 201602 (2015).
[10] X. Liu, L. Zhu, Q. Wu, and Y. Feng, "Highly-confined and low-loss spoof surface plasmon polaritons structure with periodic loading of trapezoidal grooves," AIP Adv. **5**, 077123 (2015).
[11] W. Zhang, G. Zhu, L. Sun, and F. Lin, "Trapping of surface plasmon wave through gradient corrugated strip with underlayer ground and manipulating its propagation," Appl. Phys. Lett. **106**, 021104 (2015).
[12] A. Kianinejad, Z. N. Chen, and C. W. Qiu, "Design and modeling of spoof surface plasmon modes-based microwave slow-wave transmission line," IEEE Trans. Microw. Theory Techn. **63**, 1817–1825 (2015).
[13] H. C. Zhang, Q. Zhang, J. F. Liu, W. Tang, Y. Fan, and T. J. Cui, "Smaller-loss planar SPP transmission line than conventional microstrip in microwave frequencies," Sci. Rep. **6**, 23396 (2016).
[14] X. Gao, L. Zhou, Z. Liao, H. F. Ma, and T. J. Cui, "An ultra-wideband surface plasmonic filter in microwave frequency," Appl. Phys. Lett. **104**, 191603 (2014).
[15] Q. Zhang, H. C. Zhang, H. Wu, and T. J. Cui, "A hybrid circuit for spoof surface plasmons and spatial waveguide modes to reach controllable band-pass filters," Sci. Rep. **5**, 16531 (2015).
[16] J. Y. Yin, J. Ren, H. C. Zhang, B. C. Pan, and T. J. Cui, "Broadband frequency-selective spoof surface plasmon polaritons on ultrathin metallic structure," Sci. Rep. **5**, 8165 (2015).
[17] B. C. Pan, Z. Liao, J. Zhao, and T. J. Cui, "Controlling rejections of spoof surface plasmon polaritons using metamaterial particles," Opt. Express **22**, 13940–13950 (2014).
[18] D. Martín-Cano, M. L. Nesterov, A. I. Fernandez-Dominguez, F. J. Garcia-Vidal, L. Martin-Moreno, and E. Moreno, "Domino plasmons for subwavelength terahertz circuitry," Opt. Express **18**, 754–764 (2010).
[19] Y. J. Zhou, B. J. Yang, and X. X. Yang, "A directional coupler based on spoof MIM plasmonic structures," In Proc. IEEE AP-S. Int. Symp. 354–355 (2014, July).
[20] X. Liu, Y. Feng, K. Chen, B. Zhu, J. Zhao, and T. Jiang, "Planar surface plasmonic waveguide devices based on symmetric corrugated thin film structures," Opt. Express **22**, 20107–20116 (2014).
[21] X. Gao, L. Zhou, X. Y. Yu, W. P. Cao, H. O. Li, H. F. Ma, and T. J. Cui, "Ultra-wideband surface plasmonic Y-splitter," Opt. Express **23**, 23270–23277 (2015).
[22] J. J. Xu, J. Y. Yin, H. C. Zhang, and T. J. Cui, "Compact feeding network for array radiations of spoof surface plasmon polaritons," Sci. Rep. **6**, 22692 (2016).
[23] K. Song, F. Zhang, S. Hu, and Y. Fan, "Ku-band 200-W pulsed power amplifier based on waveguide spatially power-combining technique for industrial applications," IEEE Trans. Ind. Electron. **61**, 4274–4280 (2014).
[24] S. W. Qu, D. J. He, S. Yang, and Z. Nie, "Novel parasitic micro strip arrays for low-cost active phased array applications," IEEE Trans. Antennas Propag. **62**, 1731–1737 (2014).
[25] T. H. Ho and S. J. Chung, "Design and measurement of a doppler radar with new quadrature hybrid mixer for vehicle applications," IEEE Trans. Microw. Theory Techn. **58**, 1–8 (2010).
[26] L. Zhu, S. Sun, and R. Li, "*Microwave bandpass filters for wideband communications*," New Jersey, John Wiley & Sons, (2012).
[27] Y. L. Wu, M. J. Qu, and Y. A. Liu, "A generalized lossy transmission-line model for tunable Graphene-based transmission lines with attenuation phenomenon," Sci. Rep. **6**, 31760 (2016).
[28] Y. L. Wu, Y. A. Liu, Q. Xue, S. L. Li, and C. P. Yu, "Analytical design method of multiway dual-band planar power dividers with arbitrary power division," IEEE Trans. Microw. Theory Tech. **58**, 3832–3841 (2010).